Analysis and Comprehensive Analytical Modeling of Statistical Variations in Subthreshold MOSFET's High Frequency Characteristics

Rawid BANCHUIN

Department of Computer Engineering, Faculty of Engineering, Siam University,
38 Petkasem Road, Bangkok 10160, Thailand

rawid.ban@siam.edu

Abstract. *In this research, the analysis of statistical variations in subthreshold MOSFET's high frequency characteristics defined in terms of gate capacitance and transition frequency, have been shown and the resulting comprehensive analytical models of such variations in terms of their variances have been proposed. Major imperfection in the physical level properties including random dopant fluctuation and effects of variations in MOSFET's manufacturing process, have been taken into account in the proposed analysis and modeling. The up to dated comprehensive analytical model of statistical variation in MOSFET's parameter has been used as the basis of analysis and modeling. The resulting models have been found to be both analytic and comprehensive as they are the precise mathematical expressions in terms of physical level variables of MOSFET. Furthermore, they have been verified at the nanometer level by using 65 nm level BSIM4 based benchmarks and have been found to be very accurate with smaller than 5 % average percentages of errors. Hence, the performed analysis gives the resulting models which have been found to be the potential mathematical tool for the statistical and variability aware analysis and design of subthreshold MOSFET based VHF circuits, systems and applications.*

Keywords

1. Introduction

Subthreshold region operated MOSFET has been adopted in various VHF circuits, systems and applications such as passive wireless Microsystems [1], low power receiver for wireless PAN [2], low power LNA [3], [4] and RF front-end for low power mobile TV applications [5] etc. Of course, the performances of these VHF apparatuses are mainly determined by two major high frequency characteristics of intrinsic subthreshold MOSFET entitled gate capacitance, C_g and transition frequency, f_T which is also known as unity gain frequency.

Obviously, imperfection in the physical level properties of MOSFET for example random dopant fluctuation along with those caused by variations in the manufacturing process of the device such as line edge roughness and gate length random fluctuation etc., cause the variations in MOSFET's electrical characteristics such as drain current and transconductance etc. These variations are crucial in the statistical and variability aware design of MOSFET based applications. So, there are many previous studies devoted to such variations in electrical characteristics such as [1], [6], [7], [8], [9], [10], [11], [12] which subthreshold region operated MOSFET has been focused in [1], [6], [10], [11], [12].

However, these studies did not mention anything about the variations in C_g and f_T even though they also exist and greatly affect the high frequency performances of the MOSFET based circuits and systems. By this motivation, analytical models of such variations in C_g and f_T have been performed [13], [14]. In [13], an analytical model of statistical variation in f_T as its variance expressed in term of the variance of C_g has been developed which strong inversion region operated MOSFET has been focused. Unfortunately, such model is incomprehensive as none of any related MOSFET's physical level variable has been involved. In [14], the comprehensive analytical models of random variations in C_g and f_T in term of their related MOSFET's physical level variables have been proposed where strong inversion region operated MOSFET has been focused as well. Since the subthreshold MOSFET has various applications which their performances

can be strongly influenced by variations in C_g and f_T aforementioned, studies, analyses and analytical modeling of these variations with emphasis on subthreshold MOSFET have been found to be necessary.

According to this necessity, the statistical variations in C_g and f_T of subthreshold MOSFET's have been studied and analyzed in this research. As a result, the comprehensive analytical models of these variations in terms of their variances have been proposed. Unlike previous works on variations in subthreshold MOSFET such as [1], [6], [10], [11], [12] which focus to DC characteristics, this research is focused to variations in C_g and f_T which are high frequency ones. NMOS and PMOS technologies have been separately regarded in the analysis and modeling process according to some of their unique physical level variables. Major imperfection in the physical level properties including random dopant fluctuation and those effects of variations in MOSFET's manufacturing process which yield variations in MOSFET's electrical characteristics, have been taken into account. The up to dated comprehensive analytical model of statistical variation in MOSFET's parameter [15] has been adopted as the basis of this research. The resulting models have been found to be both analytic and comprehensive as they are the precise mathematical expressions in terms of MOSFET's physical level variables. Furthermore, they have been verified at the nanometer level by using 65 nm level BSIM4 based benchmarks and have been found to be very accurate with lower than 5 % average percentages of errors. Hence, the proposed analysis and modeling gives the results which have been found to be the potential mathematical tool for the statistical and variability aware analysis and design of subthreshold MOSFET based VHF circuits, systems and applications.

2. The Proposed Analysis and Modeling

Before proceeds further, it is worthy to give some foundation on the subthreshold region operated MOSFET. Firstly, the drain current, I_d of subthreshold MOSFET can be given by

$$I_d = \mu C_{dep} \frac{W}{L} \left(\frac{kT}{q} \right)^2 \exp \left[\frac{V_{gs} - V_t}{nkT/q} \right]$$
$$\cdot \left[1 - \exp \left[-\frac{V_{ds}}{kT/q} \right] \right], \qquad (1)$$

where C_{dep} and n denote the capacitance of the depletion region under the gate area and the subthreshold parameter respectively. It should be mentioned here that the necessary condition for operating in the subthreshold region of any MOSFET is $V_{gs} < V_t$ which

can be simply given as follows [15]

$$V_t = V_{FB} + \phi_s + \epsilon_{ox}^{-1} q t_{inv} N_{sub} W_{dep}, \qquad (2)$$

where N_{sub}, t_{inv}, W_{dep}, V_{FB} and ϕ_s stand for the substrate doping concentration, electrical gate dielectric thickness, depletion width, flat band voltage and surface potential respectively.

By using Eq. (1), the transconductance, g_m of subthreshold MOSFET can be given as

$$g_m = \frac{\mu}{n} C_{dep} \frac{W}{L} \left(\frac{kT}{q} \right)^2 \exp \left[\frac{V_{gs} - V_t}{nkT/q} \right]$$
$$\left[1 - \exp \left[-\frac{V_{ds}}{kT/q} \right] \right]. \qquad (3)$$

At this point, it is ready to mention about the proposed analysis and modeling. Here, C_g can be mathematically defined as [16]

$$C_g \triangleq \frac{dQ_g}{dV_{gs}}, \qquad (4)$$

where Q_g denotes the gate charge [16] which can be given by [17]

$$Q_g = \frac{\mu W^2 L C_{ox}^2}{I_d} \int_0^{V_{gs} - V_t} (V_{gs} - V_c - V_t)^2 dV_c$$
$$- Q_{B,\max}. \qquad (5)$$

It should be mentioned here that $Q_{B,\max}$ denotes the maximum bulk charge [17]. By applying Eq. (1) for I_d in Eq. (5), Q_g of the subthreshold region operated MOSFET can be given by

$$Q_g = \frac{\left[\frac{WL^2 C_{ox}^2}{C_{dep}(kT/q)^2} \right] (V_{gs} - V_t)^3}{3 \left[1 - \exp \left[-\frac{V_{ds}}{kT/q} \right] \right] \exp \left[\frac{q}{nkT}(V_{gs} - V_t) \right]}$$
$$- Q_{B,\max}. \qquad (6)$$

So, C_g of the subthreshold MOSFET can be given as follows

$$C_g = \frac{1}{3} \left[\frac{WL^2 C_{ox}^2}{C_{dep}(kT/q)^2} \right] \left[3(V_{gs} - V_t)^2 \right.$$
$$\left. - \frac{q}{nkT}(V_{gs} - V_t)^3 \right] \exp \left[-\frac{q}{nkT}(V_{gs} - V_t) \right]. \quad (7)$$

Hence, the subthreshold MOSFET's f_T can be given by using the above equations as

$$f_T = \frac{3}{2} \left[\frac{\mu C_{dep}^2 (kT/q)^3}{2n\pi L^3 C_{ox}^2} \right] \left[1 - \exp \left[-\frac{V_{ds}}{kT/q} \right] \right]^2 \cdot$$
$$\cdot \left[\frac{\exp \left[\frac{2q}{nkT}(V_{gs} - V_t) \right]}{3(V_{gs} - V_t)^2 - \frac{q}{nkT}(V_{gs} - V_t)^3} \right]. \qquad (8)$$

By taking random dopant fluctuation and effects of variations in MOSFET's manufacturing process into account, random variations in MOSFET's parameters such as V_t, W and L etc., existed. These variations can be mathematically modeled as random variables. As an example, variation in V_t can be modeled as a random variable denoted by ΔV_t with the following variance for uniformly doped channel MOSFET [15]

$$\sigma^2_{\Delta V_t} = \frac{N_{sub}W_{dep}}{3WL} \left(\frac{qt_{inv}}{\epsilon_{ox}}\right)^2. \qquad (9)$$

Of course, ΔV_t and other variations which are also random variables e.g. ΔW, ΔL and so on, induce randomly varied C_g and f_T denoted by $C_g(\Delta V_t, \Delta W, \Delta L, \ldots)$ and $f_T(\Delta V_t, \Delta W, \Delta L, \ldots)$ respectively. So, variations in C_g and f_T which are denoted by ΔC_g and Δf_T respectively, can be mathe-

matically defined as

$$\Delta C_g \triangleq C_g(\Delta V_t, \Delta W, \Delta L, \ldots) - C_g, \qquad (10)$$

$$\Delta f_T \triangleq f_T(\Delta V_t, \Delta W, \Delta L, \ldots) - f_T. \qquad (11)$$

By using Eq. (7) and Eq. (10), ΔC_g can be given based on NMOS and PMOS technology as ΔC_{gN} and ΔC_{gP} respectively. On the other hand, Δf_T can be respectively given based on NMOS and PMOS technology by using Eq. (8) and Eq. (11) as Δf_{TN} and Δf_{TP}. After performing the analysis by mathematical formulations and approximations of various random variations in MOSFET's parameters, ΔC_{gN}, ΔC_{gP}, Δf_{TN} and Δf_{TP} can be analytically given as in Eq. (12), Eq. (13), Eq. (14) and Eq. (15), where N_a, N_d and V_{sb} denote acceptor doping density, donor doping density and source to body voltage respectively.

$$\Delta C_{gN} = 2\left[\sqrt{\frac{W}{C_{dep}}}\frac{LC_{ox}}{kT/q}\right]^2 \left[\exp\left[-\frac{V_{ds}}{kT/q}\right]-1\right]^{-1} \cdot \left[V_{gs}-V_{FB}-2\phi_F-C_{ox}^{-1}\sqrt{2q\epsilon_{Si}N_a(2\phi_F+V_{sb})}\right]$$
$$\cdot \left[V_t-V_{FB}-2\phi_F-C_{ox}^{-1}\sqrt{2q\epsilon_{Si}N_a(2\phi_F+V_{sb})}\right]. \qquad (12)$$

$$\Delta C_{gP} = 2\left[\sqrt{\frac{W}{C_{dep}}}\frac{LC_{ox}}{kT/q}\right]^2 \left[\exp\left[-\frac{V_{ds}}{kT/q}\right]-1\right]^{-1} \cdot \left[V_{gs}-V_{FB}+|2\phi_F|+C_{ox}^{-1}\sqrt{2q\epsilon_{Si}N_d(|2\phi_F|-V_{sb})}\right]$$
$$\cdot \left[V_t-V_{FB}+|2\phi_F|+C_{ox}^{-1}\sqrt{2q\epsilon_{Si}N_d(|2\phi_F|-V_{sb})}\right]. \qquad (13)$$

$$\Delta f_{TN} = \frac{\mu C_{dep}^2(kT/q)^3\left[1-\exp\left[-\frac{V_{ds}}{kT/q}\right]\right]^2}{\pi n L^3 C_{ox}^2(V_{gs}-V_{FB}-2\phi_F-C_{ox}^{-1}\sqrt{2q\epsilon_{Si}N_a(2\phi_F+V_{sb})})^3}$$
$$\cdot (V_{FB}+2\phi_F+C_{ox}^{-1}\sqrt{2q\epsilon_{Si}N_a(2\phi_F+V_{sb})}-V_t)^{-1}. \qquad (14)$$

$$\Delta f_{TP} = \frac{\mu C_{dep}^2(kT/q)^3\left[1-\exp\left[-\frac{V_{ds}}{kT/q}\right]\right]^2}{\pi n L^3 C_{ox}^2(V_{gs}-V_{FB}+|2\phi_F|+C_{ox}^{-1}\sqrt{2q\epsilon_{Si}N_d(|2\phi_F|+V_{sb})})^3}$$
$$\cdot (V_{FB}-|2\phi_F|+C_{ox}^{-1}\sqrt{2q\epsilon_{Si}N_d(|2\phi_F|+V_{sb})}-V_t)^{-1}. \qquad (15)$$

Since these variations are random variables i.e. they are nondeterministic, it is reasonable to analyze their behaviors via their statistical parameters which variance has been chosen as it is a most convenience one. By using the up to dated comprehensive analytical model of statistical variation in MOSFET's parameter

[15] as the basis without uniform channel doping profile assumption i.e. the MOSFET's channel doping profile can be non-uniform which is often in practice, the variances of these variations can be analytically formulated via statistical mathematic based analysis as

$$\sigma^2_{\Delta C_{gN}} = \frac{4q^2N_{eff}W_{dep}L}{3C_{dep}(kT/q)^2}\left[\exp\left[-\frac{V_{ds}}{kT/q}\right]-1\right]^{-2} \cdot \frac{V_t\left[V_{gs}-V_{FB}-2\phi_F-C_{ox}^{-1}\sqrt{2q\epsilon_{Si}N_a(2\phi_F+V_{sb})}\right]^2}{V_{FB}+2\phi_F+C_{ox}^{-1}\sqrt{2q\epsilon_{Si}N_a(2\phi_F+V_{sb})}}, \qquad (16)$$

$$\sigma^2_{\Delta C_{gP}} = \frac{4q^2 N_{eff} W_{dep} L}{3 C_{dep}(kT/q)^2} \left[\exp\left[-\frac{V_{ds}}{kT/q} \right] - 1 \right]^{-2}$$

$$\cdot \frac{V_t \left[V_{gs} - V_{FB} + |2\phi_F| + C_{ox}^{-1}\sqrt{2q\epsilon_{Si} N_d (2|\phi_F| - V_{sb})} \right]^2}{V_{FB} - 2|\phi_F| - C_{ox}^{-1}\sqrt{2q\epsilon_{Si} N_d (2|\phi_F| - V_{sb})}}, \tag{17}$$

$$\sigma^2_{\Delta f_{TN}} = \frac{V_t q^2 \mu^2 N_{eff} W_{dep} C_{dep}^4 (kT/q)^6 \left[1 - \exp\left[-\frac{V_{ds}}{kT/q} \right] \right]^4}{3\pi^2 n^2 W L^7 C_{ox}^6 \left[V_{FB} + 2\phi_F + C_{ox}^{-1}\sqrt{2q\epsilon_{Si} N_a (2\phi_F + V_{sb})} \right]}$$

$$\cdot \frac{1}{(V_{gs} - V_{FB} - 2\phi_F - C_{ox}^{-1}\sqrt{2q\epsilon_{Si} N_a (2\phi_F + V_{sb})})^6}, \tag{18}$$

$$\sigma^2_{\Delta f_{TP}} = \frac{V_t q^2 \mu^2 N_{eff} W_{dep} C_{dep}^4 (kT/q)^6 \left[1 - \exp\left[-\frac{V_{ds}}{kT/q} \right] \right]^4}{3\pi^2 n^2 W L^7 C_{ox}^6 \left[V_{FB} - |2\phi_F| - C_{ox}^{-1}\sqrt{2q\epsilon_{Si} N_d (2|\phi_F| - V_{sb})} \right]}$$

$$\cdot \frac{1}{(V_{gs} - V_{FB} + |2\phi_F| + C_{ox}^{-1}\sqrt{2q\epsilon_{Si} N_d (2|\phi_F| - V_{sb})})^6}, \tag{19}$$

where N_{eff} denotes the effective value of the substrate doping concentration which is now depended on the channel region depth, x as the channel doping profile is non-uniform. Let such channel region depth dependent substrate doping concentration be denoted by $N_{sub}(x)$, N_{eff} can be obtained by weight averaging of $N_{sub}(x)$ as follows

$$N_{eff} = 3 \int_0^{W_{dep}} N_{sub}(x) \left(1 - \frac{x}{W_{dep}} \right)^2 \frac{dx}{W_{dep}}. \tag{20}$$

Here, it can be seen that Eq. (16), Eq. (17), Eq. (18) and Eq. (19) are analytical expressions in terms of many related physical level variables of MOSFET. At this point, the analysis and modeling of the random dopant fluctuation and effects of MOSFET's manufacturing process variation effects induced statistical variations in subthreshold MOSFET's C_g and f_T has been completed where as their comprehensive analytical models of have been obtained as shown in Eq. (16), Eq. (17), Eq. (18) and Eq. (19) as results. These resulting models can analytically and comprehensively describe such statistical variations as they are analytical expressions in terms of many related MOSFET's physical level variables. Unlike the previous models [13], [14] which dedicate to the strong inversion region operated transistor, these models are dedicated to the subthreshold region operated MOSFET.

By using the resulting models, the statistical relationship between ΔC_g and Δf_T of any transistor which is of either N-type or P-type, can be analyzed. In order to do so, their correlation coefficient must be determined. Let A and B be random variables, their correlation coefficient denoted by ρ_{AB} can be defined as [18]

$$\rho_{AB} \triangleq \frac{E\left[(A - \overline{A})(B - \overline{B})\right]}{\sqrt{\sigma_A^2}\sqrt{\sigma_B^2}}. \tag{21}$$

After applying the models, magnitude of the desired correlation coefficient has been found to be unity for both types of MOSFET. This means that there exists a very strong statistical relationship between ΔC_g and Δf_T of any certain device.

Furthermore, variation in any crucial parameter of any subthreshold MOSFET based VHF circuit/system can be analytically formulated by using the resulting models. As a case study, analytical formulation of variation in the resulting inductance of subthreshold MOSFET based Wu current-reuse active inductor proposed in [1] will be performed. This active inductor which its original strong inversion region operated MOSFET based version has been proposed in [19], can be depicted as follows.
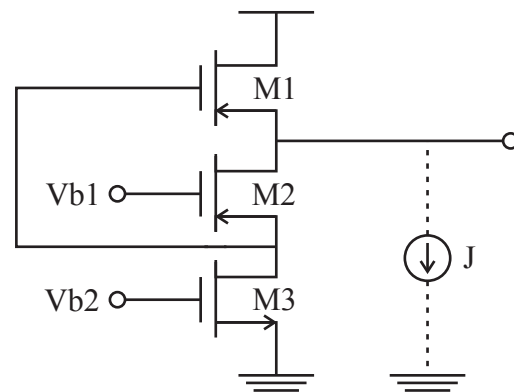

Fig. 1: Wu current-reuse active inductor [1], [19].

According to [1], the resulting inductance, L of this subthreshold MOSFET based active inductor is

$$L = \frac{C_{g1}}{g_{m1}g_{m2}}, \qquad (22)$$

where C_{g1}, g_{m1} and g_{m2} are gate capacitance of M1, transconductance of M1 and transconductance of M2 respectively.

As a result, variation in L and its variance i.e. ΔL and $\sigma_{\Delta L}^2$ can be immediately given by

$$\Delta L = \frac{\Delta C_{g1}}{g_{m1}g_{m2}}, \qquad (23)$$

$$\sigma_{\Delta L}^2 = \frac{\sigma_{\Delta C_{g1}}^2}{g_{m1}g_{m2}}, \qquad (24)$$

where ΔC_{g1} and $\sigma_{\Delta C_{g1}}^2$ are a variation in C_{g1} and its variance respectively. It can be seen that $\sigma_{\Delta L}^2$ which is of our interested can be analytically formulated by using the resulting models. This is because $\sigma_{\Delta L}^2$ is a function of $\sigma_{\Delta C_{g1}}^2$ which can be determined by applying these models to M1. Moreover, it can be observed that

$$\sigma_{\Delta L}^2 \; \alpha \; \sigma_{\Delta C_{g1}}^2, \qquad (25)$$

$$\sigma_{\Delta L}^2 \; \alpha \; \frac{1}{g_{m1}g_{m2}}. \qquad (26)$$

This means that ΔL is related to ΔC_{g1} in a directly proportional manner, so, ΔC_{g1} should be eliminated in order to prevent the occurrence of ΔL which makes the active inductor under consideration become perfectly reliable. However, ΔC_{g1} cannot be avoided in practice. So, an alternative approach has been found to be the minimizations of g_{m1} and g_{m2}.

3. Verification of the Results

In this section, the verification of these resulting models will be presented. The verifications of the resulting models obtained from the proposed analysis and modeling have been performed at the nanometer level based on 65 nm level CMOS process technology. The 65 nm level parameterized model based absolute standard deviations of ΔC_{gN}, ΔC_{gP}, Δf_{TN} and Δf_{TP} denoted by $|\sigma_{\Delta C_{gN}}|_M$, $|\sigma_{\Delta C_{gP}}|_M$, $|\sigma_{\Delta f_{TN}}|_M$ and $|\sigma_{\Delta f_{TP}}|_M$ respectively, have been graphically compared to their 65 nm level BSIM4 (SPICE LEVEL 54) based benchmarks which are respectively denoted by $|\sigma_{\Delta C_{gN}}|_B$, $|\sigma_{\Delta C_{gP}}|_B$, $|\sigma_{\Delta f_{TN}}|_B$ and $|\sigma_{\Delta f_{TP}}|_B$. It should be mentioned here that all necessary parameters have been provided by Predictive Technology Model (PTM) [20]. Furthermore, all absolute standard deviations are expressed in percentages of their corresponding nominal parameter values. Finally, W/L has been chosen to be $100/9$.

The comparative plots of the resulting model based absolute standard deviations and their benchmarks against $|V_{GS}|$ are shown in Fig. 2, Fig. 3, Fig. 4 and Fig. 5 respectively where the minimum value of $|V_{GS}|$ is 0 V and the maximum value is 0.1 V which is well below
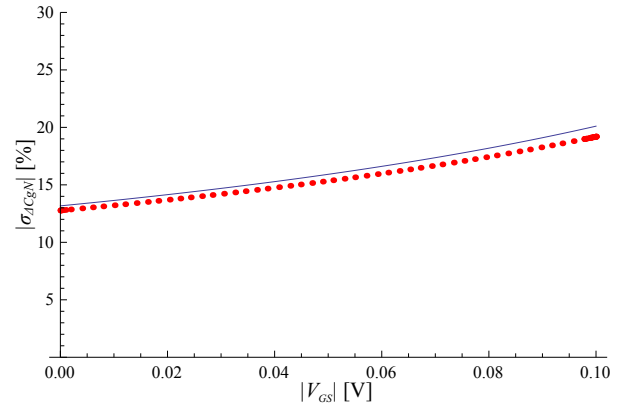

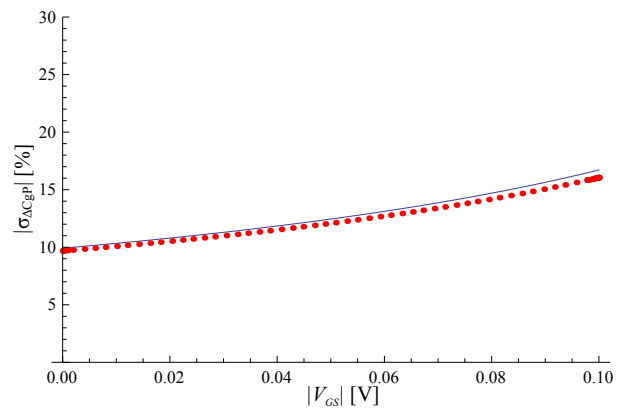**Fig. 2:** NMOS based $|\sigma_{\Delta Cg}|_M$ (line) v.s. $|\sigma_{\Delta Cg}|_B$ (dot).

Fig. 3: PMOS based $|\sigma_{\Delta Cg}|_M$ (line) v.s. $|\sigma_{\Delta Cg}|_B$ (dot).
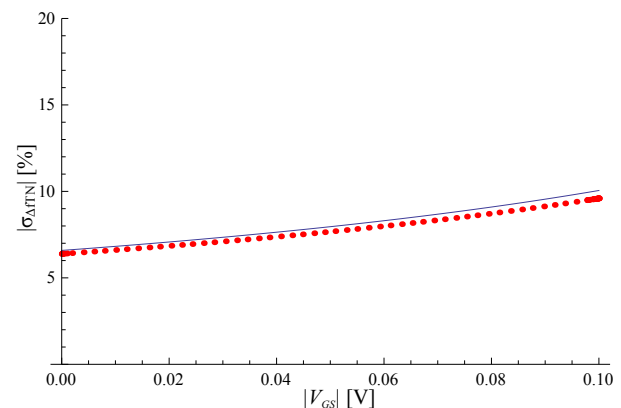

Fig. 4: NMOS based $|\sigma_{\Delta fT}|_M$ (line) v.s. $|\sigma_{\Delta fT}|_B$ (dot).

the nominal magnitude of V_t of both NMOS and PMOS transistors at 65 nm level for ensuring the subthreshold region operations. Obviously, strong agreements between the model based absolute standard deviations

and their BSIM4 based benchmarks can be observed. Furthermore, it can also be seen that absolute standard deviations of ΔC_{gP} and Δf_{TP} are respectively smaller than those of ΔC_{gN} and Δf_{TN} for all values of $|V_{GS}|$. This means that C_g and f_T of P-type MOSFET is more robust to the random dopant fluctuation and effects of variations in the manufacturing process of MOSFET than those of N-type device.
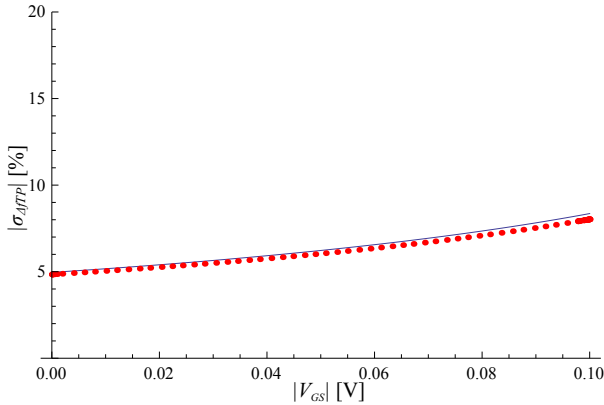

Fig. 5: PMOS based $|\sigma_{\Delta fT}|_M$ (line) v.s. $|\sigma_{\Delta fT}|_B$ (dot).

As the quantitative figure of merits of the resulting models, the average percentages of errors i.e. $\epsilon_{\Delta C_{gN},avr}$, $\epsilon_{\Delta C_{gP},avr}$, $\epsilon_{\Delta f_{TN},avr}$ and $\epsilon_{\Delta f_{TP},avr}$, have been evaluated from their corresponding comparative plots. These average percentages of errors can be generally denoted by $\epsilon_{\Delta\nu,avr}$ where $\{\Delta\nu\} = \{\Delta C_{gN}, \Delta f_{TN}, \Delta C_{gP}, \Delta f_{TP}\}$. Obviously, $\epsilon_{\Delta\nu,avr}$ can be given in terms of $|\sigma_{\Delta\nu}|_{M,i}$ and $|\sigma_{\Delta\nu}|_{B,i}$ which denote the value of $|\sigma_{\Delta\nu}|_M$ and $|\sigma_{\Delta\nu}|_B$ at any i^{th} data point respectively as follows

$$\epsilon_{\Delta\nu,avr} \triangleq \frac{1}{N_{\Delta\nu}} \sum_{i=1}^{N_{\Delta\nu}} \left[\left| \frac{|\sigma_{\Delta\nu}|_{M,i} - |\sigma_{\Delta\nu}|_{B,i}}{|\sigma_{\Delta\nu}|_{B,i}} \right| \cdot 100 \right], \quad (27)$$

where $N_{\Delta\nu}$ denotes the number of the uniformly distributed sampled data points of each of the comparative plots which is equal to each other.

With Eq. (27), it has been found that $\epsilon_{\Delta C_{gN},avr} = 3.82873$ %, $\epsilon_{\Delta C_{gP},avr} = 3.15939$ %, $\epsilon_{\Delta f_{TN},avr} = 3.7344$ % and $\epsilon_{\Delta f_{TP},avr} = 3.02822$ % which are considerably small as they are lower than 5 %. According to these pleasant quantitative figures of merits and the strong agreements seen in the comparative plots, it can be stated that the proposed analysis and modeling yield highly accurate results. Since the presented verification has been performed based on 65 nm level technology, the resulting models are obviously applicable to MOSFET in nanometer regime such as 65 nm etc.

In the subsequent section, interesting applications of these resulting models apart from those aforementioned will be shown.

4. Applications of the Results

The results obtained from the proposed analysis and modeling have various interesting applications as follows.

4.1. Motivation of the Effective Statistical and Variability Aware Designing Strategies

The effective statistical and variability aware designing strategies of the subthreshold MOSFET based VHF circuits, systems and applications can be obtained by using these resulting models. As a simple example, it can be seen from these models shown in Eq. (16), Eq. (17), Eq. (18) and Eq. (19) that

$$\sigma^2_{\Delta C_g} \; \alpha \; L, \tag{28}$$

$$\sigma^2_{\Delta f_T} \; \alpha \; L^{-7}, \tag{29}$$

where $\{\sigma^2_{\Delta C_g}, \sigma^2_{\Delta f_T}\}$ can be either $\{\sigma^2_{\Delta C_g N}, \sigma^2_{\Delta f_T N}\}$ or $\{\sigma^2_{\Delta C_g P}, \sigma^2_{\Delta f_T P}\}$ up to the type of MOSFET under consideration. So, it can be seen that even though the shrinking of gate length can reduce the ΔC_g, higher degree of increasing in Δf_T has been found to be a penalty. So, this trade-off issue must be taken into account in the designing of subthreshold region operated MOSFET based high frequency applications for any transistor type. For the statistical/variability aware design involving strong inversion region operated MOSFET, a similar trade-off can also be found since it can be seen from [14] which is dedicated to the MOSFET operated in this region that $\sigma^2_{\Delta C_g} \; \alpha \; L$ and $\sigma^2_{\Delta f_T} \; \alpha \; L^{-7}$. So, for the MOSFET of this region, shrinking of the gate length can reduce the ΔC_g with a higher degree of increasing in Δf_T as a penalty as well. However, it can be seen that such increasing in Δf_T is not as severe as that of the subthreshold MOSFET.

Let us turn our attention back to the subthreshold MOSFET which of our interested. It can also be seen from the resulting models that

$$\sigma^2_{\Delta C_g} \; \alpha \; T^{-2}, \tag{30}$$

$$\sigma^2_{\Delta f_T} \; \alpha \; T^{-6}. \tag{31}$$

It means that Δf_T is low and ΔC_g is high if the temperature is low and vice versa for high temperature. However, the rate of change in Δf_T to the temperature is greater than that of ΔC_g. Of course, this issue should be considered as well.

4.2. Bases of Subthreshold MOSFET's High Frequency Performances Optimization

The objective functions of subthreshold MOSFET's high frequency performances optimization scheme can be simply derived by using these models as bases. As an example, if such optimization scheme is of the multi objective type it may employ the following objective functions

$$\min[\sigma^2_{\Delta C_g}], \tag{32}$$

$$\min[\sigma^2_{\Delta f_T}], \tag{33}$$

where $\{\sigma^2_{\Delta C_g}, \sigma^2_{\Delta f_T}\}$ can be either $\{\sigma^2_{\Delta C_g N}, \sigma^2_{\Delta f_T N}\}$ or $\{\sigma^2_{\Delta C_g P}, \sigma^2_{\Delta f_T P}\}$ up to the type of MOSFET under consideration.

4.3. Bases of Analysis and Modeling of Variation in any High Frequency Parameter

The analysis and comprehensive analytical modeling of random dopant fluctuation and effects of manufacturing process variation induced statistical variation in any high frequency parameter of subthrehsold MOSFET, can be performed based on the resulting models where variance of such variation will be obtained as a result. In order to do so, let such high frequency parameter and its variation be denoted by X. Variation in X denoted by ΔX can be given in terms of ΔC_g and Δf_T as

$$\Delta X = \left(\frac{\partial X}{\partial C_g}\right)\Delta C_g + \left(\frac{\partial X}{\partial f_T}\right)\Delta f_T. \tag{34}$$

So, its variance i.e. $\sigma^2_{\Delta X}$ which is the desired result can be analytically given based on the already analyzed strong statistical relationship between ΔC_g and Δf_T as follows

$$\sigma^2_{\Delta X} = \left(\frac{\partial X}{\partial C_g}\right)^2 \sigma^2_{\Delta C_g} + \left(\frac{\partial X}{\partial f_T}\right)^2 \sigma^2_{\Delta f_T}$$
$$+ 2\left(\frac{\partial X}{\partial C_g}\right)\left(\frac{\partial X}{\partial f_T}\right)\sqrt{\sigma^2_{\Delta C_G}\sigma^2_{\Delta f_T}}. \tag{35}$$

Since $\{\sigma^2_{\Delta C_g}, \sigma^2_{\Delta f_T}\}$ can be either $\{\sigma^2_{\Delta C_g N}, \sigma^2_{\Delta f_T N}\}$ or $\{\sigma^2_{\Delta C_g P}, \sigma^2_{\Delta f_T P}\}$, and can be determined by using the resulting models. It should be mentioned here that both derivatives must be determined with regard to type of the transistor under consideration.

As an example, bandwidth, f_{BW} which is an often cited high frequency parameter will be considered. Obviously, f_{BW} can be given in term of gain, A and f_T by

$$f_{BW} = A^{-1}f_T. \tag{36}$$

By using the outlined principle, variation in f_{BW} and its variance i.e. Δf_{BW} and $\sigma^2_{\Delta f_{BW}}$ can be given as follows

$$\Delta f_{BW} = A^{-1}\Delta f_T, \tag{37}$$

$$\sigma^2_{\Delta f_{BW}} = A^{-2}\sigma^2_{\Delta f_T}, \tag{38}$$

where $\sigma^2_{\Delta f_T}$ can be determined by using the resulting models.

If a broader frequency spectrum must be considered i.e. a frequency parameter which is higher than f_T is of interested, the maximum oscillation frequency, $f_{\max}$ has been found to be a convenient one. According to [21], $f_{\max}$ can be given as a function of C_g and f_T under the assumption that C_g is equally divided between drain and source as

$$f_{\max} = \sqrt{\frac{f_T}{4\pi R_g C_g}}, \tag{39}$$

where R_g denotes the gate resistance of gate metallization [21] which belonged to the extrinsic part of MOSFET [22]. With the outlined principle, variation in $f_{\max}$ and its variance i.e. $\Delta f_{\max}$ and $\sigma^2_{\Delta f_{\max}}$ can be given by

$$\Delta f_{\max} = \frac{0.25}{\sqrt{\pi R_g}}\left[-\sqrt{\frac{f_T}{C_g^3}}\Delta C_g + \sqrt{\frac{1}{C_g f_T}}\Delta f_T\right], \tag{40}$$

$$\sigma^2_{\Delta f_{\max}} = \frac{0.0625 f_T}{\pi R_g C_g^3}\sigma^2_{\Delta C_g} + \frac{0.0625}{\pi R_g C_g f_T}\sigma^2_{\Delta f_T}$$
$$- \frac{0.125}{\pi R_g}\sqrt{\frac{\sigma^2_{\Delta C_g}\sigma^2_{\Delta f_T}}{C_g^3}}, \tag{41}$$

where C_g, f_T and R_g refer to their corresponding nominal values. Furthermore, $\sigma^2_{\Delta C_g}$ and $\sigma^2_{\Delta f_T}$ can be determined by the resulting models as usual.

4.4. Bases of Reduced Computational Effort Simulation of VHF Circuits, Systems and Applications

These resulting models can be mathematical bases of reduced computational effort simulation of the random dopant fluctuation and manufacturing process variation affected subthreshold MOSFET based VHF circuits, systems and applications because the standard deviation of the interested parameter of the simulated VHF circuit or system or application which is the desired outcome is a function of $\sigma^2_{\Delta C_g}$ and/or $\sigma^2_{\Delta f_T}$ which can be defined by the resulting models. If we let such interested parameter of the simulated circuit or system or application be denoted by Y, its standard deviation i.e. σ_Y can be given for any circuit or system or application with M MOSFETs as

$$\sigma_Y = \left[\sum_{i=1}^{M} \left[\left(S_{C_g}^Y |_i \right)^2 \sigma_{\Delta C_g, i}^2 + \left(S_{f_T}^Y |_i \right)^2 \sigma_{\Delta f_T, i}^2 \right] + \sum_{\substack{i=1 \\ i \neq j}}^{M} \sum_{i=1}^{M} \left[\left(S_{C_g}^Y |_i \right) \left(S_{C_g}^Y |_j \right) \rho_{\Delta C_{g,i}, \Delta C_{g,j}} \sqrt{\sigma_{\Delta C_{g,i}}^2} \sqrt{\sigma_{\Delta C_{g,j}}^2} \right. \right. \quad (42)$$

$$+ \left(S_{f_T}^Y |_i \right) \left(S_{f_T}^Y |_j \right) \rho_{\Delta f_{T,i}, \Delta f_{T,j}} \sqrt{\sigma_{\Delta f_{T,i}}^2} \sqrt{\sigma_{\Delta f_{T,j}}^2} \right] + 2 \sum_{i=1}^{M} \sum_{j=1}^{M} \left[\left(S_{C_g}^Y |_i \right) \left(S_{f_T}^Y |_j \right) \rho_{\Delta C_{g,i}, \Delta f_{T,j}} \sqrt{\sigma_{\Delta C_{g,i}}^2} \sqrt{\sigma_{\Delta f_{T,j}}^2} \right] \right]^{\frac{1}{2}},$$

where $\rho_{\Delta C_{g,i}, \Delta C_{g,j}}$, $\rho_{\Delta f_{T,i}, \Delta f_{T,j}}$ and $\rho_{\Delta C_{g,i}, \Delta f_{T,j}}$ denotes the correlation coefficient between ΔC_g of ith and j^{th} MOSFET, the similar quantity for Δf_T and the correlation coefficient between ΔC_g of ith MOSFET and Δf_T of jth MOSFET respectively. It should be mentioned here that the magnitude of $\rho_{\Delta C_{g,i}, \Delta f_{T,j}}$ can be approximated by unity when $i = j$. Furthermore, $\sigma_{\Delta C_{g,i}}^2$ and $\sigma_{\Delta f_{T,i}}^2$ denote $\sigma_{\Delta C_g}^2$ and $\sigma_{\Delta f_T}^2$ of ith MOSFET which can be either $\{\sigma_{\Delta C_{gN}}^2, \sigma_{\Delta f_{TN}}^2\}$ or $\{\sigma_{\Delta C_{gP}}^2, \sigma_{\Delta f_{TP}}^2\}$ where $\sigma_{\Delta C_{g,j}}^2$ and $\sigma_{\Delta f_{T,j}}^2$ stand for $\sigma_{\Delta C_g}^2$ and $\sigma_{\Delta f_T}^2$ of jth transistor which can be either $\{\sigma_{\Delta C_{gN}}^2, \sigma_{\Delta f_{TN}}^2\}$ or $\{\sigma_{\Delta C_{gP}}^2, \sigma_{\Delta f_{TP}}^2\}$ as well. Finally, $S_{C_g}^Y |_i$, $S_{C_g}^Y |_j$, $S_{f_T}^Y |_i$, and $S_{f_T}^Y |_j$ denote the sensitivity of Y to C_g of ith MOSFET, that to C_g of jth MOSFET, one to f_T of ith MOSFET and that to f_T of jth MOSFET respectively.

Obviously, $S_{C_g}^Y |_i$, $S_{C_g}^Y |_j$, $S_{f_T}^Y |_i$, and $S_{f_T}^Y |_j$ can be computationally determined via an efficient methodology entitled sensitivity analysis which has much lower computational effort than Monte-Carlo simulation based on the random variations of MOSFET's parameters such as V_t, W and L etc., since the simulated circuit is needed to be solved only once for obtaining these necessary sensitivities [20] then σ_Y can be immediately evaluated by using these sensitivities and the resulting models as shown in Eq. (42). On the other hand, Monte-Carlo simulation requires numerous runs in order to reach the similar outcome [23]. So, much of the computational effort can be significantly reduced by applying the resulting models and sensitivity analysis.

4.5. Bases of Analytical Modelling and Analysis of Mismatches in High Frequency Characteristics

The resulting model can be the mathematical bases of the analytical modeling and analysis of mismatches in high frequency characteristics of theoretically identical subthreshold MOSFETs even these models are dedicated to a single device. As simple illustrations, mismatches in C_g and f_T between theoretically identical MOSFETs indexed by i and j denoted by δC_{gij} and δf_{Tij} respectively will be considered.

As the analysis of any mismatch in MOSFET can be conveniently performed by using its variance [24], [25], the analysis of δC_{gij} and δf_{Tij} will be performed in this manner. Let the variances of δC_{gij} and δf_{Tij} be denoted by $\sigma_{\delta C_{gij}}^2$ and $\sigma_{\delta f_{Tij}}^2$ respectively, the analytical model of can be given in terms of $\sigma_{\Delta C_{gi}}^2$ and $\sigma_{\Delta C_{gj}}^2$ as

$$\sigma_{\delta C_{gij}}^2 = \sigma_{\Delta C_{g,i}}^2 + \sigma_{\Delta C_{g,j}}^2 - 2\rho_{\Delta C_{g,i}, \Delta C_{g,j}} \sigma_{\Delta C_{g,i}} \sigma_{\Delta C_{g,j}}. \quad (43)$$

On the other hand, that of $\sigma_{\delta f_{Tij}}^2$ can be expressed in the similar manner in terms of $\sigma_{\Delta f_{Ti}}^2$ and $\sigma_{\Delta f_{Tj}}^2$ as follows

$$\sigma_{\delta f_{Tij}}^2 = \sigma_{\Delta f_{T,i}}^2 + \sigma_{\Delta f_{T,j}}^2 - 2\rho_{\Delta f_{T,i}, \Delta f_{T,j}} \sigma_{\Delta f_{T,i}} \sigma_{\Delta f_{T,j}}. \quad (44)$$

It can be immediately seen that the analytical modeling of $\sigma_{\delta C_{gij}}^2$ can be performed by using $\sigma_{\Delta C_{gi}}^2$ and $\sigma_{\Delta C_{gj}}^2$. On the other hand, that of $\sigma_{\delta f_{Tij}}^2$ can be done by using $\sigma_{\Delta f_{Ti}}^2$ and $\sigma_{\Delta f_{Tj}}^2$. By using the obtained models of $\sigma_{\delta C_{gij}}^2$ and $\sigma_{\delta f_{Tij}}^2$, δC_{gij} and δf_{Tij} can be conveniently analyzed. Since the resulting models of this research define $\sigma_{\Delta C_{gi}}^2, \sigma_{\Delta C_{gj}}^2, \sigma_{\Delta f_{Ti}}^2$ and $\sigma_{\Delta f_{Tj}}^2$ as aforementioned, they also define and serve as the mathematical bases of analytical modeling of $\sigma_{\delta C_{gij}}^2$ and $\sigma_{\delta f_{Tij}}^2$ which yields the convenient analysis of δC_{gij} and δf_{Tij}. The examples of such analysis can be given as follows. As the correlation between closely spaced MOSFETs is very strong [24], [25], $\sigma_{\delta C_{gij}}^2$ and $\sigma_{\delta f_{Tij}}^2$ for closely spaced and positively correlated devices can be given by

$$\sigma_{\delta C_{gij}}^2 = \sigma_{\Delta C_{g,i}}^2 + \sigma_{\Delta C_{g,j}}^2 - 2\sigma_{\Delta C_{g,i}} \sigma_{\Delta C_{g,j}}, \quad (45)$$

$$\sigma_{\delta f_{Tij}}^2 = \sigma_{\Delta f_{T,i}}^2 + \sigma_{\Delta f_{T,j}}^2 - 2\sigma_{\Delta f_{T,i}} \sigma_{\Delta f_{T,j}}. \quad (46)$$

For closely spaced devices with negative correlation hand, $\sigma_{\delta C_{gij}}^2$ and $\sigma_{\delta f_{Tij}}^2$ can be determined as

$$\sigma_{\delta C_{gij}}^2 = \sigma_{\Delta C_{g,i}}^2 + \sigma_{\Delta C_{g,j}}^2 + 2\sigma_{\Delta C_{g,i}} \sigma_{\Delta C_{g,j}}, \quad (47)$$

$$\sigma_{\delta f_{Tij}}^2 = \sigma_{\Delta f_{T,i}}^2 + \sigma_{\Delta f_{T,j}}^2 + 2\sigma_{\Delta f_{T,i}} \sigma_{\Delta f_{T,j}}. \quad (48)$$

Since δC_{gij} and δf_{Tij} are respectively directly proportional to $\sigma_{\delta C_{gij}}^2$ and $\sigma_{\delta f_{Tij}}^2$, it can be observed from Eq. (45), Eq. (46), Eq. (47) and Eq. (48) that δC_{gij} and δf_{Tij} are maximized when MOSFETs are closely spaced with negative correlation and minimized for those closely spaced and positively correlated devices.

Now, distanced MOSFETs will be considered. For such devices, $\sigma^2_{\delta C_{gij}}$ and $\sigma^2_{\delta f_{Tij}}$ become

$$\sigma^2_{\delta C_{gij}} = \sigma^2_{\Delta C_{g,i}} + \sigma^2_{\Delta C_{g,j}}, \tag{49}$$

$$\sigma^2_{\delta f_{Tij}} = \sigma^2_{\Delta f_{T,i}} + \sigma^2_{\Delta f_{T,j}}. \tag{50}$$

This is because the correlation between distanced devices can be neglected as it is very weak [24] so, it cannot affect δC_{gij} and δf_{Tij} as can be seen from Eq. (49) and Eq. (50) which have no correlation related terms.

If it is assumed that all transistors under consideration are statistically identical i.e. $\sigma^2_{\Delta C_{g,i}} = \sigma^2_{\Delta C_{g,j}} = \sigma^2_{\Delta C_g}$ and $\sigma^2_{\Delta f_{T,i}} = \sigma^2_{\Delta f_{T,j}} = \sigma^2_{\Delta f_T}$ where $\{\sigma^2_{\Delta C_g}, \sigma^2_{\Delta f_T}\}$ can be either $\{\sigma^2_{\Delta C_{gN}}, \sigma^2_{\Delta f_{TN}}\}$ or $\{\sigma^2_{\Delta C_{gP}}, \sigma^2_{\Delta f_{TP}}\}$ as usual, $\sigma^2_{\delta C_{gij}}$ and $\sigma^2_{\delta f_{Tij}}$ can be simplified as follows

$$\sigma^2_{\delta C_{gij}} = 2\sigma^2_{\Delta C_g}(1 - 2\rho_{\Delta C_{g,i}, \Delta C_{g,j}}), \tag{51}$$

$$\sigma^2_{\delta f_{Tij}} = 2\sigma^2_{\Delta f_T}(1 - 2\rho_{\Delta f_{T,i}, \Delta f_{T,j}}). \tag{52}$$

Obviously, $\sigma^2_{\delta C_{gij}}$ and $\sigma^2_{\delta f_{Tij}}$ for closely spaced and positively correlated devices can be approximated as $\sigma^2_{\delta C_{gij}} = 0$ and $\sigma^2_{\delta f_{Tij}} = 0$. This means that δC_{gij} and δf_{Tij} for statistically identical, closely spaced and positively correlated devices can be neglected.

5. Conclusion

In this research, the analysis of statistical variations in subthreshold MOSFET's C_g and f_T, have been shown. As a result, the comprehensive analytical models of these variations in terms of their variances have been proposed. Both random dopant fluctuation and effects of variations in MOSFET's manufacturing process have been taken into account in the proposed analysis and modeling. The up to dated comprehensive analytical model of statistical variation in MOSFET's parameter [15] has been adopted as the basis. The resulting models have been found to be very accurate according to their pleasant verification results with less than 5 % average percentages of errors. They also have various applications for examples analytical study of random variation in crucial parameter of subthreshold MOSFET based VHF circuit/system e.g. variation in L of subthreshold MOSFET based Wu current-reuse active inductor [1] etc., and being the mathematical basis for various interesting tasks such as the optimization of subthreshold MOSFET's high frequency characteristic, analytical modeling of the mismatches in these characteristics and sensitivity analysis based simulation of any VHF circuit, system and application involving subthreshold MOSFET which is be more computationally efficient than the Monte-Carlo simulation

[23], etc. Hence, the analysis and modeling proposed in this research gives the results which have been found to be the convenient analytical tool for the statistical and variability aware analysis and design of various subthreshold MOSFET based VHF circuits, systems and applications.

Acknowledgment

References

[1] YUSHI, Z. and F. YUAN. Subthreshold CMOS active inductor with applications to low-power injection-locked oscillators for passive wireless Microsystems. In: *53rd IEEE International Midwest Symposium on Circuits and System (MWSCAS), 2010.* Seattle: IEEE, 2010, pp. 885–888. ISBN 978-1-4244-7771-5. DOI: 10.1109/MWSCAS.2010.5548661.

[2] BEVIN, G., P., R. MUKHOPADHYAY, S. CHAKRABORTY, C.-H. LEE and J. LASKAR. A Low Power Fully Monolithic Subthreshold CMOS Receiver with Integrated LO Generation for 2.4 GHz Wireless PAN Application. *IEEE Journal of Solid-State Circuits.* 2008, vol. 43, iss. 10, pp. 2229–2238. ISSN 0018-9200. DOI: 10.1109/JSSC.2008.2004330.

[3] BEVIN G., P., S. CHAKRABORTY, C.-H. LEE and J. LASKAR. A Fully Monolithic 260-μW, 1-GHz Subthreshold Low Noise Amplifier. *IEEE Microwave and Wireless Components Letters.* 2005, vol. 15, iss. 6, pp. 428–430. ISSN 1531-1309. DOI: 10.1109/LMWC.2005.850563.

[4] HANIL, L. and S. MOHAMMADI. A 3GHz Subthreshold CMOS Low Noise Amplifier. In: *IEEE Radio Frequency Integrated Circuits (RFIC) Symposium, 2006.* San Francisco: IEEE, 2006, pp. 494–497. ISBN 0-7803-9572-7. DOI: 10.1109/RFIC.2006.1651199.

[5] SEONGDO, K., J. CHOI, J. LEE, B. KOO, C. KIM, N. EUM, H. YU and H. JUNG. A Subthreshold CMOS Front-End Design for Low-Power Band-III T-DMB/DAB Recievers. *ETRI Journal.* 2011, vol. 33, no. 6, pp. 969–972. ISSN 1225-6463. DOI: 10.4218/etrij.11.0211.0055.

[6] HIROO, M., T. KIDA and S.-I OHKAWA. Comprehensive Matching Characterization of Analog CMOS Circuits. *IEICE Transaction on Fundamentals of Electronics, Communications and*

Computer Sciences. 2009, vol. E92-A, no. 4, pp. 966–975. ISSN 0916-8508. DOI: 10.1587/transfun.E92.A.966.

[7] RAWID, B. Process Induced Random Variation models of Nanoscale MOS Performance: Efficient Tool for The Nanoscale Regime Analog/Mixed Signal CMOS Statistical/Variability Aware Design. In: *International Conference on Information and Electronics Engineering 2011*. Bangkok: IACSIT Press, 2011, pp. 6–12. ISBN 978-981-08-8637-0.

[8] RAWID, B. Complete Circuit Level Random Variation Models of Nanoscale MOS Performance. *International Journal of Information and Electronic Engineering.* 2011, vol. 1, iss. 1, pp. 9–15. ISSN 2010-3719. DOI: 10.7763/IJIEE.2011.V1.2.

[9] LU, W. and S. LING LING. Modeling of Current Mismatch Induced by Random Dopant Fluctuation. *Journal of Semiconductors.* 2011, vol. 32, iss. 8, pp. 1–6. ISSN 1674-4926. DOI: 10.1088/1674-4926/32/8/084003.

[10] KOSTAS, P. A Designer's Approach to Device Mismatch: Theory, Modeling, Simulation Techniques, Scripting, Applications and Examples. *Analog Integrated Circuits and Signal Processing.* 2006, vol. 48, iss. 2, pp. 95–106. ISSN 0925-1030. DOI: 10.1007/s10470-006-5367-2.

[11] RAJEEV, R., A. SRIVASTAVA, D. BLAAUW and D. SYLVESTER. Statistical Analysis of Subthreshold Leakage Current for VLSI Circuits. *IEEE Transactions on Very Large Scale Integration (VLSI) Systems.* 2004, vol. 12, iss. 2, pp. 131–139. ISSN 1063-8210. DOI: 10.1109/TVLSI.2003.821549.

[12] FRANCESCO, F. and M. E. WRIGHT. Measurement of MOS current mismatch in the weak inversion region. *IEEE Journal of Solid-State Circuits.* 1994, vol. 29, iss. 2, pp. 138–142. ISSN 0018-9200. DOI: 10.1109/4.272119.

[13] HAN-SU, K., C. CHUNG, J. LIM, K. PARK, H. OH and H.-K. KANG. Characterization and modeling of RF-performance (fT) fluctuation in MOSFETs. *IEEE Electron Device Letters.* 2009, vol. 30, iss. 8, pp. 855–857. ISSN 0741-3106. DOI: 10.1109/LED.2009.2023826.

[14] RAWID, B. Novel Complete Probabilistic Models of Random Variation in High Frequency Performance of Nanoscale MOSFET. *Journal of Electrical and Computer Engineering.* 2013, vol. 2013, iss. 189436, pp. 1–10. ISSN 2090-0147. DOI: 10.1155/2013/189436.

[15] KIYOSHI, T., A. NISHIDA and H. TOSHIRO. Random Fluctuations in Scaled MOS Devices. In: *International Conference on Simulation of Semiconductor Processes and Devices 2009*. San Diego: IEEE, 2009, pp. 1–7. ISBN 978-1-4244-3974-8. DOI: 10.1109/SISPAD.2009.5290243.

[16] ABEBE, H., H. MORRIS, E. CUMBERBATCH and V. TYREE. Compact Gate Capacitance Model with Polysilicon Depletion Effect for MOS Device. *Journal of Semiconductor Technology and Science.* 2007, vol. 7, no. 2, pp. 209–213. ISSN 1598-1657.

[17] HOWE, R. T. and C. G. SODINI. *Microelectronics: An Integrated Approach.* Upper Saddle River: Prentice Hall, 1996. ISBN 978-0-135-88518-5.

[18] HINES, W. W., D. C. MONTGOMERY, D. M. GOLDMAN and C. M. BORROR. *Probability and Statistics in Engineering.* 4th ed. Chichester: Wiley, 2003. ISBN 978-0-471-24087-7.

[19] YEU, W., X. DING, M. ISMAIL and H. K. OLSSON. RF bandpass filter design based on CMOS active inductors. *IEEE Transaction on Circuits and Systems II: Analog and Digital Signal Processing.* 2003, vol. 50, iss. 12, pp. 942–949. ISSN 1057-7130. DOI: 10.1109/TCSII.2003.820235.

[20] Predictive Technology Model. *Nanoscale Integration and Modeling (NIMO) Group* [online]. 2011. Available at: `ptm.asu.edu`.

[21] PULFREY, D. L. *Understanding Modern Transistors and Diodes.* 1st ed. Cambridge: Cambridge University press, 2010. ISBN 978-0-521-51460-6.

[22] CHENG, Y., M. J. DEEN and C.-H. CHEN. MOSFET modeling for RF IC design. *IEEE Transactions on Electron Devices.* 2005, vol. 52, iss. 7, pp. 1286–1303. ISSN 0018-9383. DOI: 10.1109/TED.2005.850656.

[23] CIJAN, G., T. TUMA and A. BURMEN. Modeling and Simulation of MOS Transistor Mismatch. In: *6th Eurosim Congress on Modeling and Simulation.* Ljubljana: ARGE Simulation News, 2007, pp. 1–8. ISBN 978-3-901608-32-2.

[24] CATHIGNOL, A., S. MENILLO, S. BORDEZ, L. VENDRAME and G. GHIBAUDO. Spacing Impact on MOSFET Mismatch. In: *IEEE International Conference on Microelectronic Test Structure 2008*. Edinburgh: IEEE, 2009, pp. 90–95. ISBN 978-1-4224-1800-8. DOI: 10.1109/ICMTS.2008.4509320.

[25] MEZZOMO, C. M., A. BAJOLET, A. CATHIGNOL, R. DI FRENZA and G. GHIBAUDO. Characterization and Modeling of Transistor

Variability in Advanced CMOS Technologies. *IEEE Transactions on Electron Devices*. 2011, vol. 58, iss. 8, pp. 2235–2248. ISSN 0018-9383. DOI: 10.1109/TED.2011.2141140.

About Authors

Rawid BANCHUIN was born in 1976. He received his Ph.D. Electrical and Computer Engineering from King Mongkut University of Technology Thonburi, Thailand in 2008. His research interests include application of fractional calculus in electrical and electronic engineering, fractional impedance, nanoscale CMOS circuits, systems and technologies, variability in CMOS circuits and systems, mathematical modeling of mixed signal circuits and systems, on-chip inductor and on-chip transformer.